RSC Advances

ROYAL SOCIETY OF CHEMISTRY

www.rsc.org/advances

RSC Advances

ARTICLE

Separation of fluorine/cerium from fluorine-bearing rare earth sulfate solution by selective adsorption using hydrous zirconium oxide

Received 00th February 2016,

Accepted 00th February 2016

DOI: 10.1039/x0xx00000x

www.rsc.org/

Jingui He,[a,b] Yong Li,[a] Xiangxin Xue ,[a,*] Hongqiang Ru,[b] Xiaowei Huang [c] and He Yang [a]

Abstract: Separation of fluorine/cerium from fluorine-bearing rare earth sulfate solution by coordination adsorption was studied using hydrous zirconium oxide as an adsorbent. The relevant parameters studied for fluoride adsorption were the effects of contact time, pH, n_F/n_{Ce} ratio, initial fluoride concentratin and coexisting ions. The material was characterized by XRD, SEM,EDS, Raman, FTIR and XPS. The Raman, FTIR and XPS spectra suggest that an ion-exchange reaction between hydroxyl ion on hydrous zirconium oxide and fluoride is involved. The most of the fluoride adsorption takes place in the first 3min. The adsorption capacities of fluoride and cerium both increase with increase in solution pH, and the optimum pH is suggested to be 0.3-0.6. The loss of cerium is higher at low n_F/n_{Ce} ratio. High initial fluoride concentration is unfavorable for the separation. The accompanied rare earth ions have no significant influence on adsorption of fluoride. The adsorbed fluoride can be desorbed effectively with 0.1mol·l^{-1} NaOH which shows utility of the adsorbent in a sustainable manner. In addition, the effectiveness of the method was also evaluated using real bastnaesite sulfuric acid leaching solution. This work represented a potential use of hydrous zirconium oxide for adsorption and separation of fluorine from cerium in fluorine-bearing rare earth sulfate solution and it is expected to eliminate the influence of fluorine on the extraction separation of rare earths.

1 Introduction

Bastnaesite($ReCO_3F$, Re=Rare earths) is one of the most important mineral resources containing about 50 wt% cerium, 0.2–0.3 wt% thorium and 8-10 wt% fluorine.[1,2] There are several hydrometallurgical methods to extract rare earths from bastnaesite. Recently, the main technology for bastnaesite treatment is “oxidation roasting - acid leaching - solvent extraction”. According to the selectivity in the separation of rare earth elements, type of gangue minerals in the ore and the reagents to be used in the further extraction procedures, the sulfuric, hydrochloric and nitric acids can be chosen as leaching reagents.[3] The sulfuric acid leaching process can dissolve almost all of Ce^{4+}, RE^{3+} and F^-, which makes the resources in bastnaesite fully utilized. It is considered to be more advanced technology for bastnaesite comprehensive utilization in the future.[4-7]

During the process of bastnasite treatment, some issues still remain. Bastnaesite theoretically contains about 8~10% fluorine. Due to its high electronegativity and small ionic size, the fluoride ion mainly exists in the form of $[CeF_2]^{2+}$ and REF_3 complexes in sulfuric acid system,[8-10] which makes it difficult to extract Ce^{4+} and RE^{3+}, and brings about the formation of the third phase in the extraction process. Therefore, the key point of sulfuric acid leaching process is to eliminate the influence of fluorine. Lots of investigations about defluorination in the hydrometallurgical process of bastnaesite have been reported.[11-14] In recent years, the most commonly used methods for fluoride removal are adsorption,[15,16] reverse osmosis,[17] ion exchange,[18] precipitation,[19] etc. Adsorption has been found to be the most important one for easy operation, affordable cost and water quality.[20] A large number of materials have been studied as adsorbents, such as activated alumina,[21,22] activated carbon,[23] bone char,[24] clay[25] and zeolite[26]. The amorphous hydrous zirconium oxide has been known to have a remarkable selectivity to fluoride ion, and has attracted attention for defluorination due to the simplicity of preparation, the large surface area and the strong regeneration capacity.[27-30] It can be used for defluoridation of groundwater and industrial wastewater. To our knowledge, the systemic study of fluoride removal in the refining of bastnaesite by hydrous zirconium oxide has not been seen yet.

In this paper, we chose the hydrous zirconium oxide as adsorbent due to its applicability in strong acidic solution. The hydrous zirconium oxide was prepared by precipitation, and the separation of fluorine/cerium from fluorine-bearing rare earth sulfate solution by selective adsorption onto hydrous zirconium oxide has been studied. The objective of this paper is mainly to eliminate the influence of fluorine on the extraction separation of rare earths.

2 Experimental

2.1 Materials

Sulfuric acid(98%), sodium fluoride(NaF), cerium sulfate tetrahydrate ($Ce(SO_4)_2$•$4H_2O$), zirconium oxychloride($ZrOCl_2$·$8H_2O$),

[a] School of Metallurgy, Northeastern University, Shenyang, Liaoning 110819, China.
[b] School of Material Science and Engineering, Northeastern University, Shenyang, Liaoning 110819, China.
[c] National Engineering Research Center for Rare Earth Materials, General Research Institute for Nonferrous Metals, and Grirem Advanced Materials Co., Ltd.,Beijing 100088,China.
† *Corresponding author: Email: Xue_Xiangxin@126.com (X. Xue).

lanthanum oxide(La_2O_3), praseodymium oxide(Pr_6O_{11}), neodymium oxide(Nd_2O_3), samarium oxide(Sm_2O_3), etc. of analytical grade were purchased from Shenyang Guoyao Group Chemical Reagent Co., Ltd. All of the chemicals were diluted with deionized water.

The mineral samples of bastnaesite used in this work were obtained from the Sichuan Mianning mine in China.

2.2 Instruments

NOVA 1200e surface area & pore size analyzer (Quantachrome) was used to analyze the BET surface area and pore size distribution by N_2 adsorption at 77K. A BT-9300H laser scattering particle analyzer (Bettersize Instruments Ltd.) was used to detect the particle size distribution of product. Ultima Ⅳ X-ray diffraction (Rigaku) was used to examine the phase structure in the 2θ of 10-80°at a rate of 8°min^{-1} with Cu Kα radiation. S-3400N scanning electron microscope (Hitachi) with an energy dispersive spectrum (EDS) technique was used to detect the surface atomic composition of adsorbent. The Nicolet-380 fourier transform infrared spectrometer (Thermo Electron Corporation) was used to detect the chemical structure of the product, and the preparation of the sample consisted in dispersing and gently grinding the powder in KBr. HR800UV laser Raman spectrometer (Horibajobin Yvon) was used to record the Raman spectra of product in the range of 100-1000 cm^{-1} using the excitation wavelength of 325nm at a resolution of 2 cm^{-1}. The ESCALAB250 X-ray photoelectron spectroscopy (XPS) (Thermo VG) with an Al Kα excitation source (1486.6eV) was used to examine the surface chemical composition of samples. A C1s calibration energy of 284.6eV was used as reference to corrected the XPS results. The XPS data were fitted using a nonlinear least-square curve fitting program (XPSPEAK41 software).

PXSJ-216 ion meter connected with a PF-1 fluoride ion electrode and saturated calomel electrode (Shanghai Precision Scientific Instrument Co., Ltd.) was used to determine the electric potential of fluoride. The PHS-3C digital pH meter connected with an E-201-C pH electrode (Shanghai Precision Scientific Instrument Co., Ltd.) was used to detect the pH values of solutions. HY-4 speed control multi-use oscillator (Jiangsu Jintan Dadi Automation Instrument Plant) was used to carry out the adsorption experiments.

2.3 Synthesis of hydrous zirconium oxide

The hydrous zirconium oxide was prepared by dissolution of 25g zirconium oxychloride in deionized water. Excess of ammonium hydroxide solution (1:1) was slowly added dropwise to the solution with stirring magnetically at 60℃ until the pH reached 8~9, and the precipitate obtained was hydrous zirconium oxide. After precipitation, it was activated at 65~70℃ with constant stirring for 2h, then filtered and washed several times with distilled water until free of Cl^-. The product was dried in an oven at 100~110℃ until a constant weight was achieved, then ground for detection.[31]

2.4 Batch adsorption experiments with synthetic solution

The **synthetic** fluoride stock solution was prepared by dissolution of cerium sulfate tetrahydrate, sodium fluoride, rare earth oxides and sulfuric acid in deionized water and further diluted to the desired concentration for practical use. All adsorption studies were carried out by mixing known weight of adsorbent material with 100ml of fluorine-bearing rare earth sulfate solution in a plastic bottle. The mixture was stirred thoroughly at room temperature, and then the sample was filtered with 0.45μm filter. The filtrate was then analyzed for fluoride and other ions concentrations. The experiments variables considered were: (1) contact time between adsorbent and solution, 0~6min; (2) pH of solution, 0~1; (3) n_F/n_{Ce} ratio, 1~2; (4) initial fluoride concentration, 0.5~8 g·l^{-1}; (5)coexisting rear earth ions, La^{3+}, Pr^{3+}, Nd^{3+},Sm^{3+}.

Cerium concentration was determined by titration with standard $(NH_4)_2Fe(SO_4)_2$ using sodium diphenylamine sulfonate as indicator. Trivalent rare earth concentrations were determined by titration with standard EDTA using xylenol orange as indicator. Zirconium concentration was determined by thermal titration with standard EDTA with xylenol orange as the indicator under HNO_3 condition, and using aluminum salt as fluorine complexing agent, hydroxylamine hydrochloride as Ce^{4+} reducing agent. Fluoride concentration was analyzed with a fluoride-selective electrode connected to an ion meter. Before determination, total ionic strength adjusting buffer (TISAB) was added to solution in order to maintain ionic strength and the pH, and eliminate the interference effect of complexing ions.

2.5 Adsorption experiment using real bastnaesite sulfuric acid leaching solution

The effectiveness of the method was also evaluated using real bastnaesite sulfuric acid leaching solution. The water sample was collected from the sulfuric acid leaching of roasted bastnaesite. The typical concentration ranges in sulfuric acid leaching solution are CeO_2 (15~50g·l^{-1}), CeO_2/REO (47~50%), F (0.5~8g·l^{-1}), C_H^+ (0.2~3mol·l^{-1}) and other trace elements. The n_F/n_{Ce} ratio is about 1~2. The adsorption and separation experiments were conducted with varying the adsorbent dose from 5 to 30g·l^{-1} of the sample by the batch process. The hydrous zirconium oxide of a definite amount was added in 100ml sulfuric acid leaching solution sample, and mixed well by a mechanical stirrer. The filtrate was analyzed for fluoride and cerium concentrations.

2.6 Desorption and Regeneration

The desorption and regeneration of the fluoride-loaded hydrous zirconium oxide was performed following a sequence of 1st to 5th cycle of batch operation study. The sample was treated in sodium hydroxide solution (pH=13) at room temperature for 4h with a solid/solution ratio of 1:5~10 under stirring. Then sample was filtered, washed several times with deionized water, and dried in an oven at 100~110℃ for 1~2h.The regenerated hydrous zirconium oxide was attained. The fluoride concentration in the filtered solutions was analyzed to calculate desorption ratio.

2.7 Equation

The adsorption rate η (%), adsorption capacity q_t (mg·g^1) and distribution coefficient D (ml·g^1) were calculated as following expression:

$$\eta = \frac{c_i - c_f}{c_i} \times 100\% \quad (1)$$

$$q_t = \frac{(c_i - c_f) \times V}{m} \quad (2)$$

$$D = \frac{c_i - c_f}{c_f} \times \frac{V}{m} \quad (3)$$

where c_i denotes the initial ion concentrations in solution, g·l^{-1}; c_f denotes the final ion concentrations, g·l^{-1}; V denotes the volume of solution, ml; m denotes the mass of the adsorbent material, g.

3 Results and discussion

3.1 Characterization of adsorbent

The specific surface area and the average micropore diameter of the adsorbent determined by BET technique were found to be 171.53m^2/g and 3.41nm. The particle size distribution of the hydrous zirconium oxide is given in Fig.1. The mean diameter of adsorbent is about 16.82μm.

The X-ray diffraction pattern of synthesized hydrous zirconium oxide is shown in Fig.2. No crystalline peak is detected in the pattern, indicating the amorphous characteristics of the material. The surface morphology of hydrous zirconium oxide before and after adsorption is shown in Fig.3. The micrographs show that the hydrous zirconium oxide has a significantly rougher surface with lots of pores, indicating that the adsorbent is porous. Compared with hydrous zirconium oxide, the fluoride-adsorbed adsorbent has smaller particles and less pores. The corresponding EDS spectrum shows the elemental composition of fluoride-loaded hydrous zirconium oxide. The presence of F signal reveals that fluoride is successfully adsorbed on hydrous zirconium oxide.

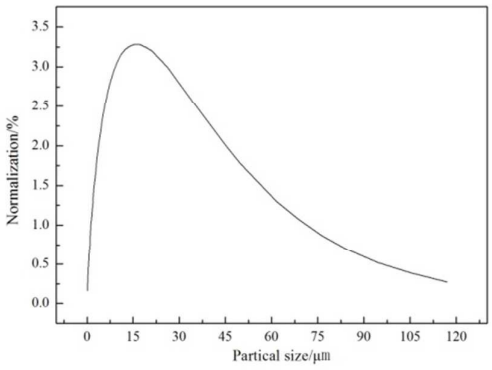

Fig. 1. Particle size distribution of hydrous zirconium oxide.

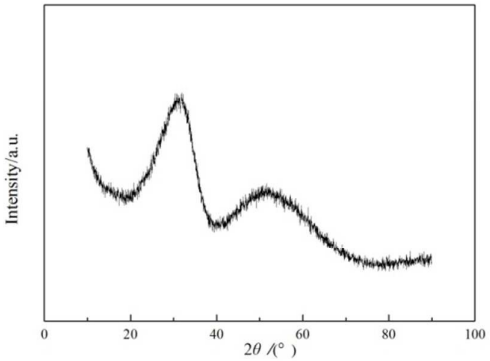

Fig. 2. X-ray diffraction pattern of prepared hydrous zirconium oxide.

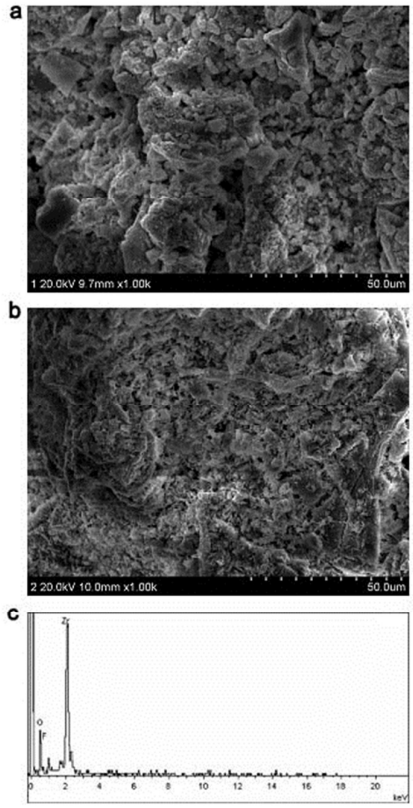

Fig. 3. SEM images of the hydrous zirconium oxide before (a) and after (b) adsorption and (c) EDX spectrum of fluoride-adsorbed material.

3.2 Mechanism of fluoride adsorption

The Raman spectra of hydrous zirconium oxide before and after adsorption are shown in Fig.4. The shape of the spectra indicates a amorphous structure which is consistent with X-ray diffraction pattern. The broad band at 533 cm^{-1} is due to the bridging-hydroxy perpendicular-to-plane Zr-O stretch.[32] The bands at 207 cm^{-1} and 400 cm^{-1} are indicative for Raman-active mode for ZrO_2.[33] Both of the characteristic bands weakened after fluoride adsorption, indicating a chemisorption process involving between hydrous zirconium oxide and fluoride. The time dependence is also shown in Fig.4. It is observed that the fluoride adsorption is a fast process and can take place within 10min.

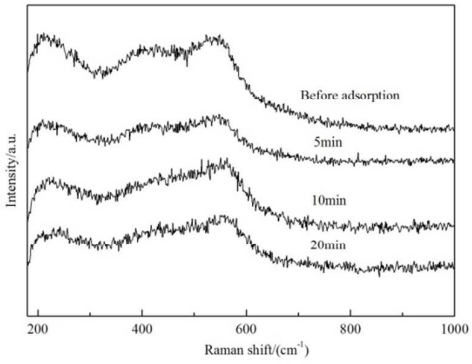

Fig. 4. Raman spectra of hydrous zirconium oxide before and after adsorption with laser excitation at 325nm.

The FTIR spectra of hydrous zirconium oxide before and after adsorption are presented in Fig.5. The peaks at 3573 and 3469 cm^{-1} are attributed to the symmetric and asymmetric stretching modes of molecular water coordinated to the hydrous zirconium oxide and the bending vibration of the –OH bonds of chemisorbed water.[34] The peak at 3415cm^{-1} is due to the stretching modes of -OH bonds related to free water adsorbed on the surface of the adsorbent. The peak at 1625cm^{-1} is due to the bending modes of H-O-H bonds. The peak observed at 470cm^{-1} is assigned to the Zr-O bonds in ZrO_2.[35] The peak at 1353cm^{-1} [36,37] is for the bending vibration of Zr-OH groups which decreases significantly after fluoride sorption. This evidence indicates that fluoride has replaced a substantial fraction of –OH groups bound to zirconium. The peak at 1125 cm^{-1} can be assigned to the adsorbed SO_4^{2-} groups. It is also found from the spectra that the intensity of Zr-OH peak decreases sharply in the initial 5min, and has no evident change with time go on, which indicates that the adsorption of fluoride on hydrous zirconium oxide is a very fast process.

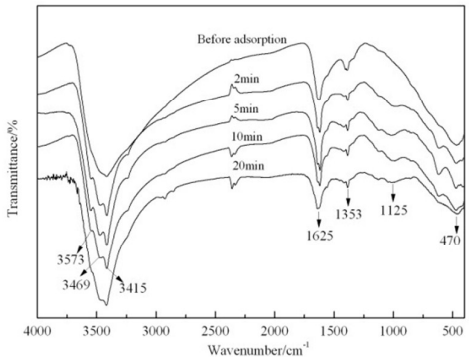

Fig. 5. FTIR spectra of hydrous zirconium oxide before and after adsorption.

To further investigate the interactions between fluoride and hydrous zirconium oxide, XPS studies of hydrous zirconium oxide before and after adsorption were conducted and the results are displayed in Fig.6-8. The mechanism between fluoride and functional groups on hydrous zirconium oxide can be concluded through the characteristic peak shift and intensity change in XPS spectra. As shown in Fig.6, a strong F1s peak at 685.5eV is found after adsorption,[27] clearly indicating the surface reactions have occurred between fluoride and zirconium. Fig.7 gives the O1s XPS spectra before and after adsorption. For the original adsorbent, the O1s peak can be fitted into two peaks at 529.8 and 531.6eV, which are assigned to Zr-O groups and Zr-OH groups, respectively.[38] After adsorption, the Zr-O and Zr-OH peaks shift to a higher binding energy by about 0.5eV and 0.3eV. This must be due to the formation of new zirconium species. The area ratio of the Zr-OH peak decreases from 63.2 to 39.4%, while the area ratio of the Zr-O peak increases from 36.8 to 60.6%, suggesting that the hydroxyl groups on the hydrous zirconium oxide surface surely participated in fluoride sorption, which is consistent with the result of the FTIR spectra.

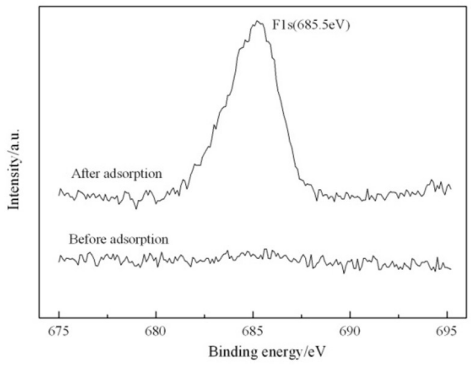

Fig. 6. F1s core-level spectra of hydrous zirconium oxide before and after adsorption.

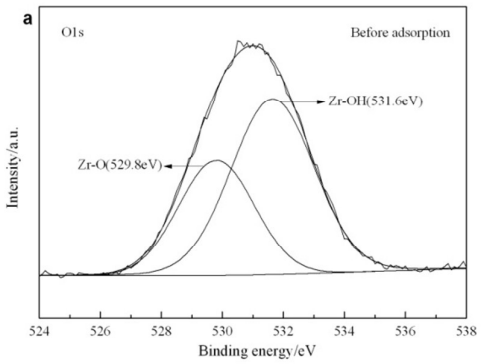

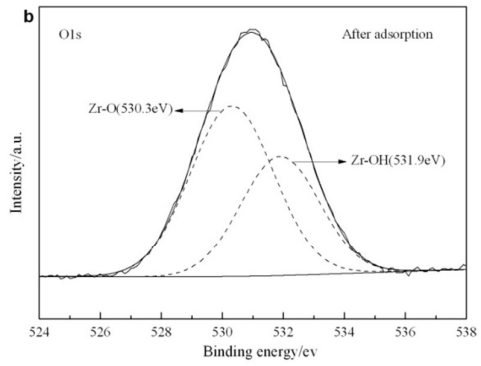

Fig. 7. F O1s core-level spectra of hydrous zirconium oxide before and after adsorption.

Fig.8 shows the Zr3d XPS spectra before and after adsorption. The prominent peaks in the spectra before adsorption at 182.1 and 184.4eV can be attributed to $Zr3d_{5/2}$ and $Zr3d_{3/2}$, which broadened and shifted to a higher binding energy by about 0.3eV after adsorption. This is what would be expected when zirconium becomes bonded to fluorine. Bonding to fluorine causes the loss of electron density at zirconium, which in turn raises $Zr3d_{5/2}$ and $Zr3d_{3/2}$ binding energies. [27] The deconvoluted Zr3d spectra of the adsorbent after adsorption is exhibited in Fig.8(b) as two

overlapped peaks for both $Zr3d_{3/2}$ and $Zr3d_{5/2}$. The new peaks at 182.9 and 184.9eV can be attributed to Zr-oxyfluoride species. The similar results have been reported by previous study.[27,39,40]

According to above results, the mechanism is supported with the evidence of FTIR and XPS spectra for the involvement of -OH group in fluoride adsorption. The most probable reaction is given as:

$$\text{-Zr-OH}_{(s)}+F^-_{(aq)} \rightleftarrows \text{-Zr-F}_{(s)}+OH^-_{(aq)} \quad (4)$$

It has been reported that F^- coordinates with Ce^{4+} to form $[CeF_2]^{2+}$ complex in fluorine-bearing rare earth sulfate solution at high acidity.[9] The hydrous zirconium oxide can take the F^- from $[CeF_2]^{2+}$, leading to the separation of fluorine and cerium. The separation mechanism can be described by the reaction below:

$$2\ \text{-Zr-OH}_{(s)}+[CeF_2]^{2+}_{(aq)} \rightleftarrows 2\ \text{-Zr-F}_{(s)}+Ce^{4+}_{(aq)}+2\ OH^-_{(aq)} \quad (5)$$

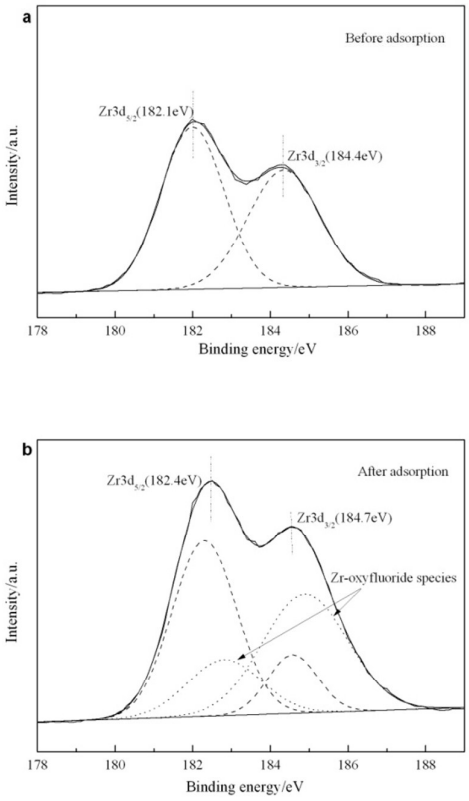

Fig. 8. Zr3d core-level spectra of hydrous zirconium oxide before and after adsorption.

3.3 Batch adsorption experiments with synthetic solution

3.3.1Effect of contact time

According to the Raman and FTIR analyses, the fluoride adsorption is a fast process. The effect of contact time on the separation of fluorine and cerium was conducted within 10min.

Fig.9 depicts the effect of contact time on the variation of adsorption rates of fluoride and cerium. It is observed that most of the fluoride adsorption takes place in the first 3min. This could be attributed to the availability of high surface area as well as porous structural facilitating the adsorption of fluoride. The cerium adsorption is about 0 during the whole process, indicating that hydrous zirconium oxide possesses strong selective absorption capacity to fluoride in F-Ce solution. In addition, there was a possibility that some of the hydrous zirconium oxide dissolved in acid solution, so the concentration of zirconium was measured after the adsorption, and the results are shown in Fig.9. The dissolved amount is quite low in initial 5min of the reaction but increases with increase in time, so 3min is chosen as the period of contact time for further studies.

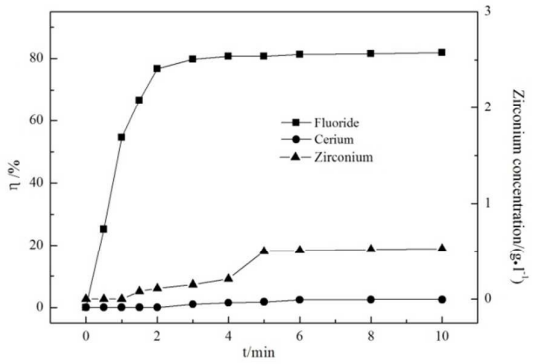

Fig. 9. The effect of contact time on separation of fluoride and cerium (concentration of fluoride: $1g{\cdot}l^{-1}$; n_F/n_{Ce}: 2; pH: 0.3; adsorbent dose: $10g{\cdot}l^{-1}$).

3.3.2 Effect of solution pH

The solution pH is one of the most important parameters which directly influence the existing state of cerium and the characteristics of adsorbent. It is reported that cerium only exist in the form of Ce^{4+} at pH 1.0 or lower, and $[Ce(OH)]^{3+}$, $[Ce(OH)]^{2+}$ or $[CeO]^{2+}$ at higher pH value .[41,42] Therefore, the effect of solution pH on separation of fluorine and cerium from fluorine-bearing rare earth sulfate solution was examined over the pH range of 0 to1 and the results are illustrated in Table 1. The results show that the adsorption capacities of fluoride and cerium both increase with increase in solution pH. The dissolved amount of hydrous zirconium oxide increases with rise of solution acidity as shown in Fig.10, leading to the decrease of fluoride adsorption amount. The high D_{Ce} at pH around 0.8 can be attributed to the strong hydrolysis property of cerium at lower acidity, which leads to the loss of cerium. Shifts of pH before and after adsorption were also observed. The pH of the treated solutions increased. The mechanism of fluoride adsorption by hydrous zirconium oxide was thought to be anion exchange between available surface -OH group and fluoride. The increased pH after adsorption can be attributed to the liberation of hydroxyl ion on hydrous zirconium oxide. This can also be supported by the evidences of FTIR and XPS spectra.

To obtain the high separation efficiency with lower dissolved amount of hydrous zirconium oxide, the optimum pH is suggested to be 0.3-0.6.

Table 1 The effect of initial pH on separation of fluoride and cerium (concentration of fluoride: $1g{\cdot}l^{-1}$; n_F/n_{Ce}: 2; adsorbent dose: $10g{\cdot}l^{-1}$).

Initial pH	η/%		q_t/ (mg·g^1)		D/ (ml·g^1)	
	F	Ce	F	Ce	F	Ce
0.00	67.23	0.00	67.23	0.00	205.18	0.00
0.12	68.20	0.00	68.20	0.00	214.46	0.00
0.32	68.98	1.68	68.98	6.21	222.41	1.71
0.61	72.59	9.28	72.59	34.25	264.80	10.23
0.82	74.7	50.10	74.77	184.50	296.29	100.00

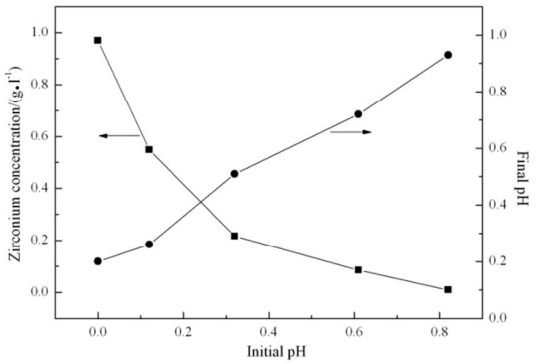

Fig. 10. The effect of initial pH on dissolution of adsorbent and the variation of final pH against initial pH.

3.3.3 Effect of n_F/n_{Ce}

The n_F/n_{Ce} ratio is an important parameter of fluorine-bearing rare earth sulfate solution which affects the complex state of fluoride and cerium. The effect of n_F/n_{Ce} ratio on the separation of fluorine and cerium was investigated as shown in Table 2. It is found that the adsorption capacities of fluoride and cerium decrease with increasing n_F/n_{Ce} from 1 to 2. Theoretically, the hydrous zirconium oxide has no adsorption ability for cerium, but there are some residual free Ce^{4+} at low n_F/n_{Ce} ratio which will enter the skeleton and channel of hydrous zirconium oxide by mechanical mixing,[43] resulting in the loss of cerium. With increase in n_F/n_{Ce} ratio, F^- and Ce^{4+} exist mainly as $[CeF_2]^{2+}$ complex, and few free Ce^{4+} is left in solution, leading to less loss of cerium and high separation efficiency of fluorine and cerium. As shown in Fig.11, the release of zirconium is in an acceptable range and has a slight rise with increase of n_F/n_{Ce}, which probably because the uptake of cerium can reduce the dissolution of hydrous zirconium oxide.

Table 2 The effect of n_F/n_{Ce} ratio on separation of fluoride and cerium (concentration of fluoride: 1g·l^{-1}; pH: 0.3; adsorbent dose: 10g·l^{-1}).

n_F/n_{Ce}	η/%		q_t/ (mg·g^{-1})		D/ (ml·g^{-1})	
	F	Ce	F	Ce	F	Ce
1.0	81.49	9.98	81.49	73.58	440.37	11.09
1.2	80.15	8.35	80.15	51.35	403.78	9.11
1.5	79.55	4.47	79.55	22.00	389.03	4.68
1.8	78.54	3.29	78.54	13.49	366.15	3.40
2.0	77.98	2.23	77.98	8.22	334.52	2.28

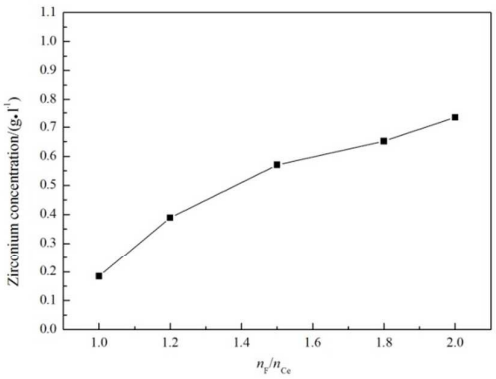

Fig. 11. The effect of n_F/n_{Ce} ratio on dissolution of adsorbent.

3.3.4 Effect of initial fluoride concentration

The effect of initial fluoride concentration on the separation of fluorine and cerium is shown in Table 3. It is noticed that the adsorption rate and distribution coefficient of fluoride decrease sharply with the increase of initial fluoride concentration, while the adsorption capacity of fluoride increases. This may because that at a fixed dose of adsorbent, the adsorption on the surface is saturated faster at higher concentration of fluoride showing a higher q_e value.[44] Additionally, the dissolved amount of zirconium gradually increases with increasing in fluoride concentration as shown in Fig.12. This may be because that the high fluoride concentration promotes the formation of HF, and HF can exist in the solution destroying the Zr–O–Zr bonding of hydrous zirconium oxide.[45] This result shows that high initial fluoride concentration is unfavorable for the separation. The optimum concentration should be less than 5g·l^{-1}.

Table 3 The effect of initial concentration of fluoride on separation of fluoride and cerium(n_F/n_{Ce}: 2; pH: 0.3; adsorbent dose: 15g·l^{-1}).

Initial concentration of fluoride	η/%		q_t/ (mg·g^{-1})		D/ (ml·g^{-1})	
	F	Ce	F	Ce	F	Ce
0.5	85.86	0.00	28.62	0.00	405.01	0.00
1.0	85.15	0.00	56.77	0.00	382.25	0.00
2.0	84.16	4.87	112.21	23.92	354.15	3.41
3.0	80.33	6.74	160.67	49.72	272.33	4.82
4.0	77.11	7.69	205.61	75.69	224.52	5.56
5.0	69.98	7.78	233.28	95.71	155.43	5.63
6.0	65.72	2.73	262.87	40.24	127.80	1.87
7.0	51.92	1.48	242.31	25.43	72.00	1.01
8.0	45.48	0.00	242.55	0.00	55.61	0.00

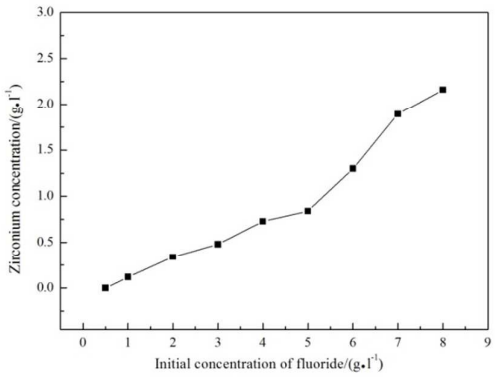

Fig. 12. The effect of initial concentration of fluoride on dissolution of adsorbent.

3.3.5 Effect of coexisting rare earth ions

A variety of other rare earths are generally accompanied with cerium in fluorine-bearing rare earth sulfate solution, such as La, Pr, Nd and Sm. The influence of coexisting rare earth ions on adsorption of fluorine and the separation of fluorine and rare earths were investigated. The results are shown in Table 4. The RE^{3+} ions were prepared by dissolving certain amount of their oxides in solution, and were equimolar with cerium. It is found that the distribution coefficients of fluoride and cerium are almost stable, and the hydrous zirconium oxide has no adsorption for RE^{3+}, implying that the accompanied ions have no significant influence on adsorption of fluorine, and it is possible to separate fluorine and rare earths from fluorine-bearing rare earth sulfate solution using hydrous zirconium oxide because of the high selectivity and anti-interference ability for fluoride.

Table 4 The effect of coexisting rare earth ions on separation of fluoride and cerium(concentration of fluoride: 1g·l^{-1} ; n_F/n_{Ce}: 2; pH: 0.3; adsorbent dose: 10g·l^{-1}).

RE^{3+}	η/%			q_t/ (mg·g^{-1})		D/ (ml·g^{-1})	
	F	Ce	RE	F	Ce	F	Ce
La	76.51	1.96	0.00	76.51	7.23	325.60	2.01
Pr	77.12	1.09	0.00	77.12	4.01	337.12	1.16
Nd	75.89	3.28	0.00	75.89	12.13	314.73	3.45
Sm	77.31	1.67	0.00	77.31	6.16	340.85	1.74

3.4 Experiment using real bastnaesite sulfuric acid leaching solution

The main components of the used bastnaesite sulfuric acid leaching solution sample estimated were CeO_2 32.71 g·l^{-1}, CeO_2/REO 48.25%, F 4.96 g·l^{-1}, C_H^+ 2mol·l^{-1}. The pH of the water sample was adjusted to be 0.3 with ammonium hydroxide. The synthetic solution was also prepared according to the composition of realistic solution. The effect of adsorbent dose on separation of fluorine and cerium from synthetic and realistic solution samples was studied as shown in Fig.13. It is apparent that the higher adsorbent dose corresponds to the higher distribution coefficient of fluoride. This agrees well with the increase of solid dose for a fixed solute, and surface sites heterogeneity of the adsorbent.[44] The distribution coefficient of cerium is extremely low when the dose below 20 g·l^{-1}, but obviously increase when the dose above 20 g·l^{-1}. Thus, the good separation of fluorine and cerium can be obtained at the adsorbent dose of 20 g·l^{-1} with higher distribution coefficient of fluoride and lower loss of cerium.

Besides, higher distribution coefficient is obtained from synthetic solution in comparison to realistic bastnaesite sulfuric acid leaching solution. The reason could be due to the fact that real solution is always associated with large number of cations and anions, which could interfere with the normal adsorption process.[46]

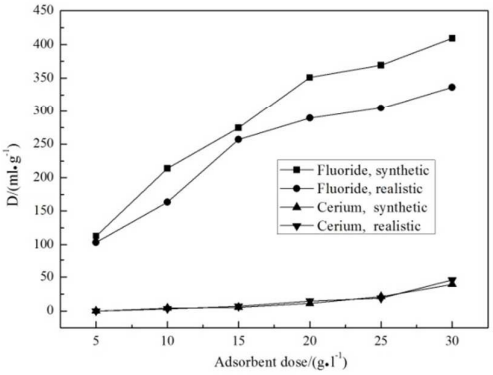

Fig. 13. The separation of fluoride and cerium in synthetic and realistic solution samples with varying adsorbent dose.

3.5 Desorption and Regeneration

The regenerated ability is an important factor for an advanced adsorbent, and the cost can be reduced if the adsorbent regenerated and reused in many cycles of operation. The desorption experiments of fluoride-adsorbed hydrous zirconium oxide were performed using 0.1mol • l^{-1} NaOH solution as regeneration fluid.[44] The EDS pattern of regenerated zirconium oxide is shown in Fig.14. The absence of F element in EDS spectrum reveals that the fluoride can be desorbed effectively with a desorption ratio reaching 91%. A fluoride adsorption experiments was also performed with original and regenerated hydrous zirconium oxide. The results are shown in Fig.15. After five cycles of desorption-adsorption process, the regenerated hydrous zirconium oxide material can still show high adsorption ability just with a little reduction.

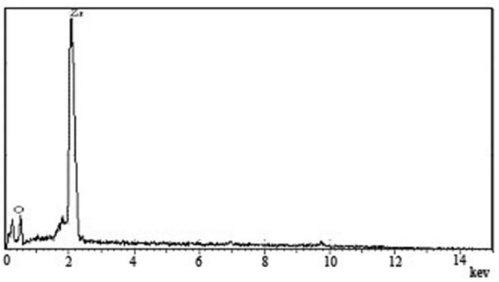

Fig. 14. The EDS pattern of regenerated adsorbent.

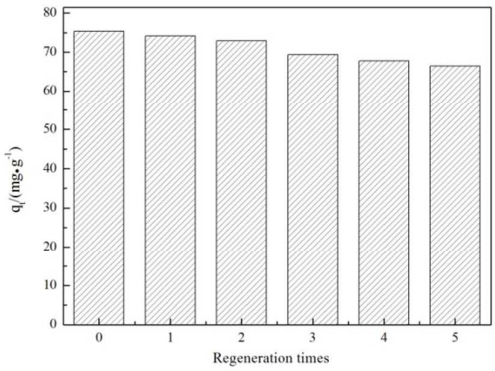

Fig. 15. Regeneration test of hydrous zirconium oxide.

4 Conclusions

In this study, amorphous hydrous zirconium oxide prepared by precipitation was used for adsorption and separation of fluorine from cerium in fluorine-bearing rare earth sulfate solution. The adsorbent was characterized by XRD, SEM and EDS. The batch adsorption studies show that: the most of the fluoride adsorption takes place in the first 3min; the adsorption capacities of fluoride and cerium both increase with increase in solution pH, and the optimum pH is suggested to be 0.3-0.6; the loss of cerium is higher at low n_F/n_{Ce} ratio; high initial fluoride concentration is unfavorable for the separation; the accompanied rare earth ions have no significant influence on adsorption of fluorine. A possible mechanism of adsorption process involving an ion-exchange reaction between hydroxyl ion on hydrous zirconium oxide and fluoride is proposed basing on Raman, FTIR and XPS studies. The effectiveness of the method was also evaluated using real bastnaesite sulfuric acid leaching solution. The adsorbed fluoride can be desorbed effectively using 0.1mol·l^{-1} NaOH with desorption ratio reaching 91%, and adsorbent can sustainably be utilized for a number of cycles. This work represented a potential use of hydrous zirconium oxide for adsorption and separation of fluorine from cerium in fluorine-bearing rare earth sulfate solution and hence it is expected to eliminate the influence of fluorine on the extraction separation of rare earths.

Acknowledgements

The financial aids from the following programs are gratefully acknowledged. They are the key program of National Natural Science Foundation of China (NSFC: 50934004), National Natural Science Foundation of China (51274061), Major State Basic Research Development Program of China (973 Program: 2012CBA01205), Fundamental Research Supporting Project of Northeastern University (N110602006).

References

1 G.X. Xu, Rare Earths, second ed., Metallurgical Industry Press, Beijing, 1995, 377-399. (In chinese)
2 M. Kul, Y. Topkaya., İ. Karakaya, Hydrometallurgy, 2008, 93, 129-135.
3 G.M. Ritcey, A.W. Ashbrook, Amsterdam, 1979, 386- 420.
4 X.W. Huang, Z.Q. Long, H.W. Li, W.J. Ying, G.C. Zhang, X.X. Xue, J. Rare Earths, 2005, 23, 1-4.
5 S.L. Zhao, C.G. He, Z.J. Cao, Y. Liu, F. Zhao, Chin. Rare Earths, 2003, 24, 32-35. (In chinese)
6 Q.W. Zhang, F. Saito, Hydrometallurgy, 1998, 47, 231-241.
7 A.Yörükoğlu, A. Obut, İ. Girgin, Hydrometallurgy,2003, 68, 195-202.
8 R.M. Sawant, R.K. Rastogi, M.A. Mahajan, N.K. Chaudhuri, Talanta, 1996, 43, 89-94.
9 J. Qiao, C.R. Zhang, S.G. Liu, X.K. Hao, Chin. Rare Earths, 1997, 18, 64-67. (In chinese)
10 Z.F. Zhang, H.F. Li, F.Q. Guo, S.L. Meng, D.Q. Li, Sep. Purif. Technol, 2008, 63, 348-352.
11 X.H. Luo, X.W. Huang, Z.W. Zhu, Z.Q. Long, Y. Liu, J. Rare Earths, 2009, 27, 119-122.
12 J.N. Li, X.W. Huang, Z.W. Zhu, Z.Q. Long, X.L. Peng, D.L. Cui, J. Rare Earths, 2007, 25, 55-58.
13 X.W. Huang, J.N. Li, Z.Q. Long, Y.Q. Zhang, X.X. Xue, Z.W. Zhu, J. Rare Earths, 2008, 26, 410-413.
14 Z.Q. Long, X.W. Huang, W.M. Huang, G.C. Zhang, J. Chin. Rare Earths Sci., 2000, 18, 18-20.
15 Y. Ku, H.M. Chiou, Water Air Soil Pollut., 2002, 133, 349-360.
16 X.P. Liao, B. Shi, Environ. Sci. Technol., 2005, 39, 4628-4632.
17 S.V. Joshi, S.H. Mehta, A.P. Rao, A.V. Rao, Water Treat., 1992, 10, 307-312.
18 Y. Ku, H.M. Chiou, W. Wang, Sep. Sci. Technol.,2002, 37, 89-103.
19 M. Yang, Y. Zhang, B. Shao, R. Qi, H. Myoga, J. Environ. Eng., 2001, 127, 902-907.
20 Meenakshi, R.C. Maheshwari, J. Hazard. Mater., 2006, 137, 456-463.
21 S. Ghorai, K.K. Pant, Sep. Purif. Technol., 2005, 42, 265-271.
22 R.S. Wang, H.M. Li, W. Feng, J. Environ. Sci., 1992, 12(3), 333-339.
23 Y.H. Li, S.G. Wang, X.F. Zhang, J.Q. Wei, C.L. Xu, Z.K. Luan, D.H. Wu, Mater. Res. Bull., 2003, 38, 469-476.
24 N.A. Medellin-Castillo, R. Leyva-Ramos, R. Ocampo-Perez, R.F. Garcia de la Cruz, A. Aragon-Piña, J.M. Martinez-Rosales, R.M. Guerrero-Coronado, L.Fuentes-Rubio, Ind. Eng. Chem. Res., 2007, 46, 9205-9212.
25 M. Mahramanlioglu, I. Kizilcikli, I.O. Bicer, J. Fluorine Chem., 2002, 115, 41-47.
26 M.S. Onyango, T.Y. Leswifi, A. Ochieng, D. Kuchar, F.O. Otieno, H. Matsuda, Ind. Eng. Chem. Res., 2008, 48, 931-937.
27 X.M. Dou, D. Mohan, C.U. Pittman Jr., S. Yang, Chem.Eng.J., 2012, 198-199, 236-245.
28 J.A. Blackwell, P.W. Carr, J. Chromatogr., 1991, A 549, 43-57.
29 K. Biswas, D. Bandhoyapadhyay, U. Ghosh, Adsorption, 2007, 13, 83-94.
30 Y.B. Sun, Q.H. Fang, J.P. Dong, X.W. Cheng, J.Q. Xu, Desalination, 2011, 277, 121-127.
31 R. Chitrakar, S. Tezuka, A. Sonoda, K. Sakane, K. Ooi, T. Hirotsu, J. Colloid Interface Sci., 2006, 297, 426-433.
32 P. Southon, University of Technology, Sydney, 2000.
33 X. Zhao, D. Vanderbilt, Phys. Rev. B 65,2002, 075105.
34 J.M. Pan, X.H. Zou, X. Wang, W. Guan, Y.S. Yan, J. Han, Chem. Eng. J., 2010, 162, 910-918.
35 S.K. Swain, S. Mishra, T. Patnaik, R.K. Patel, U. Jha, R.K. Dey, Chem. Eng. J., 2012, 184, 72-81.
36 M.L. Toullec, C.J. Simmons, J.H. Simmons, J. Am. Ceram. Soc., 1988, 71, 219-224.
37 H.L. Liu, X.F. Sun, C.Q. Yin, C. Hu, J. Hazard. Mater., 2008, 151, 616-622.

38 A. Roustila, J. Chêne, C. Séverac, Int. J. Hydrogen Energ., 2007, 32, 5026-5032.
39 S.D. Wolter, J.R. Piascik, B.R. Stoner, Appl. Surf. Sci., 2011, 257, 10177-10182.
40 C.G. Pantano, R.K. Brow, J. Am. Ceram. Soc., 1988, 71, 577-581.
41 P.H. Tedesco, V.B. De Rumi, J.A. González Quintana, J. Inorg. Nucl. Chem., 1967, 29, 2813-2817.
42 Y. Liu, Z.Q. Long, W.M. Huang, G.C. Zhang, X.W. Huang, J. Rare Earths, 2001, 19, 320-323.
43 H.R. Chen, J.L. Shi, L. Wang, T.D. Chen, J.N. Yan, D.S. Yan, J. Chin. Ceram. Soc., 2001, 29, 18-20.
44 K. Biswas, K. Gupta, U.C. Ghosh, Chem. Eng. J., 2009, 149, 196-206.
45 C.F. Chang, C.Y. Chang, T.L. Hsu, Desalination, 2011, 279, 375-382.
46 S.k. Swain, R.K. Dey, M.Islam, R.K. Patel, U. Jha, T. Patnaik, C. Airoldi, Sep. Sci. Technol., 2009, 44, 2096-2116.

$$2\text{ -Zr-OH}_{(s)}+[CeF_2]^{2+}_{(aq)} \rightleftarrows 2\text{ -Zr-F}_{(s)} +Ce^{4+}_{(aq)}+2\ OH^{-}_{(aq)}$$

The formula shows that the hydrous zirconium oxide can take the F^- from $[CeF_2]^{2+}$, leading to the separation of fluorine and cerium.